

Aloin promotes A549 cell apoptosis via the reactive oxygen species-mitogen activated protein kinase signaling pathway and p53 phosphorylation

LI WAN*, LIN ZHANG*, KAI FAN and JIANJUN WANG

Department of Thoracic Surgery, Union Hospital, Tongji Medical College, Huazhong University of Science and Technology, Wuhan, Hubei 430022, P.R. China

Received March 30, 2016; Accepted March 6, 2017

DOI: 10.3892/mmr.2017.7379

Abstract. Aloin has the potential to be a novel anticancer agent in cancer therapies. However, the detailed anticancer effect of Aloin remains to be fully elucidated. The present study analyzed the p53-dependent mechanisms in response to Aloin treatment. Using the p53-proficient A549 cells, an Aloin-induced apoptotic cell model was established, which was used to evaluate the potential underlying molecular mechanisms. The results demonstrated that 200, 300 and 400 μ M Aloin induced intrinsic cell apoptosis, which was further confirmed by disruption of the mitochondrial membrane potential, elevation of cytosolic Ca^{2+} levels, and activation of B-cell lymphoma 2 (Bcl-2) homologous antagonist killer, Bcl-2 X-associated protein, p53 upregulated modulator of apoptosis and phorbol-12-myristate-13-acetate-induced protein 1. Aloin-induced apoptosis was also accompanied by the induction of p53 phosphorylation on Serine (Ser)15, Threonine 18, Ser20 and Ser392; however, there were no significant differences in the expression of p53 and mouse double

minute 2 homolog. Aloin-induced apoptosis was reactive oxygen species (ROS)- and c-Jun/p38-dependent, as specific inhibitors for ROS, phosphorylated (p)-c-Jun and p-p38 may attenuate Aloin-induced A549 cell proliferating inhibition. In conclusion, these results suggested that Aloin may induce apoptosis in A549 cells via the ROS-mitogen activated protein kinase signaling pathway, with p53 phosphorylation. These results implicate Aloin as a potential therapeutic agent for the treatment of lung cancer.

Introduction

Aloe, an important medicinal herb, has long been used in traditional Chinese medicine to treat and cure a number of diseases. Aloin ($C_{21}H_{22}O_9$; Fig. 1A), an anthrocylic glycoside compound, is one of the primary active ingredients (15 to 40%) in aloe plant juice (1). Aloin has exhibited anti-angiogenesis, anti-inflammatory, antimicrobial and antiviral pharmacological effects (2). In addition, Aloin has been demonstrated to reduce cell proliferation and induce cell apoptosis in different human tumor cells, including Jurkat T-cells, HeLaS3 human cervical cancer cells and A549 human lung cancer cells (3,4). Therefore, Aloin may be effective as a novel anticancer agent. However, the anticancer effect of Aloin remains to be fully elucidated.

p53 serves a pivotal role in controlling cell cycle progression and cell apoptosis, which is central to its function as a tumor suppressor (5-8). In resting cells, p53 is a short-lived protein that is highly regulated and maintained at low or undetectable levels, due to degradation via the ubiquitin proteasome signaling pathway (5). A number of intracellular and extracellular stressors, including irradiation, chemicals, oxygen-free radicals, hypoxia and very low nucleotide levels, lead to rapid activation of the p53 protein (9,10). Under these conditions, the p53 protein may be rescued from degradation, accumulate to high levels and become phosphorylated on its N-terminal activation sites (11). Among these phosphorylated sites, phosphorylation of Serine (Ser)15 and 20 have been revealed to be essential for the stabilization, induction and transactivation functioning of p53. In addition, phosphorylation of Ser392 is responsible for the nuclear import of p53. Phosphorylation of Threonine 18 (Thr18) is crucial

Correspondence to: Professor Jianjun Wang, Department of Thoracic Surgery, Union Hospital, Tongji Medical College, Huazhong University of Science and Technology, 13 Hangkong Road, Wuhan, Hubei 430022, P.R. China
E-mail: wanliwh2000@sina.com

Abbreviations: MDM2, mouse double minute 2; ATM, ataxia telangiectasia mutated; ATR, ataxia-telangiectasia and Rad3 related; MAPKs, mitogen-activated protein kinases; ERK, extracellular signal-regulated kinases; TAD, N-terminal trans-activation domain; XIAP, X-linked inhibitor of apoptosis protein; DMEM, Dulbecco's modified Eagle's medium; FBS, fetal bovine serum; FITC, fluorescein isothiocyanate; PI, propidium iodide; PVDF, polyvinylidene fluoride; MMP, measurement of mitochondrial membrane potential; ROS, reactive oxygen species; H2DCF-DA, dichlorodihydrofluorescein diacetate

*Contributed equally

Key words: Aloin, p53 phosphorylation, reactive oxygen species, c-Jun, p38

for regulating interactions between p53 and its regulatory partner mouse double minute 2 (MDM2) and specific genes, including AIP1, are induced only when p53 is phosphorylated on Ser46 (12-16). Phosphorylation of p53 may be mediated by numerous cellular kinases, including ataxia telangiectasia mutated gene (ATM), ataxia-telangiectasia and Rad3 related (ATR), DNA-dependent protein kinase (DNA-PK) and the mitogen-activated protein kinases (MAPKs), including p38, c-Jun N-terminal kinase and extracellular signal-regulated kinases (ERK) (17-21).

In addition to phosphorylation, p53 protein may also be regulated by the E3 ubiquitin ligase, MDM2, which binds to the N-terminal transactivation domain (TAD) of p53 and inhibits its transcriptional activities, targeting itself and p53 for degradation by the proteasome (22). There is a large body of evidence that suggests that MDM2 has a number of p53-independent effects. One previous study revealed that MDM2 binds to and ubiquitinates the retinoblastoma protein, resulting in its degradation and the release of E2F1, which in turn promotes cell cycle progression (11). Other studies have demonstrated that MDM2 may physically interact with the internal ribosome entry site of the X-linked inhibitor of apoptosis protein (XIAP) 5'-untranslated region, resulting in translation of the latter, which generates resistance to cancer therapy (11,23,24). Therefore, targeting MDM2 itself or the MDM2-p53 interaction, may improve outcomes of cancer therapy.

Following activation, p53 stimulates a large network of signals that function through two major apoptotic pathways: The extrinsic and intrinsic pathways. The former involves regulators of cluster of differentiation (CD)95 (also known as Fas), which in turn leads to a cascade of caspase activation, including caspase-3, -8, -9 and -10. The extrinsic pathway involves regulators of CD95, caspase-8 and -10, and proapoptotic effectors of B-cell lymphoma 2 (Bcl-2) homologous antagonist killer (BAK), Bcl-2 X-associated protein (BAX), p53 upregulated modulator of apoptosis (PUMA) and phorbol-12-myristate-13-acetate-induced protein 1 (NOXA), which govern mitochondria-dependent cell apoptosis (25-27).

A previous study indicated that Aloin can induce apoptosis in p53 proficient A549 cells and p53 deficient H1299 cells. In addition, the A549 cells were more susceptible to Aloin-induced apoptosis than H1299 cells, suggesting the involvement of p53 in Aloin-induced apoptosis (28). The aim of the present study was to analyze the p53-dependent mechanisms involved in response to Aloin treatment. Using the p53-proficient A549 cells, an Aloin-induced apoptotic cell model was established. Subsequently, the potential underlying molecular mechanisms were evaluated. The results indicated that Aloin triggered the generation of reactive oxygen species (ROS), which in turn activated c-Jun and p38-p53 molecular pathways, and subsequently induced apoptosis via the intrinsic apoptotic pathway.

Materials and methods

Reagents. Dulbecco's modified Eagle's medium (DMEM), fetal bovine serum (FBS), the TRIzol[®] RNA purification kit and Fluo-4 probe were obtained from Invitrogen; Thermo Fisher Scientific, Inc. (Waltham, MA, USA). The ROS inhibitor

(2R, 4R)-4-aminopyrrolidine-2,4-dicarboxylic acid (APDC) was supplied by Enzo Life Sciences, Inc. (Farmingdale, NY, USA). The dichlorodihydrofluorescein diacetate (H₂DCF-DA) probe was purchased from Thermo Fisher Scientific, Inc. MTT, Aloin and rhodamine 123 were purchased from Sigma-Aldrich; Merck KGaA (Darmstadt, Germany). The commercial kits for protein isolation and Bicinchoninic acid (BCA) protein quantification were products of Bio-Rad Laboratories, Inc. (Hercules, CA, USA). An annexin V-fluorescein isothiocyanate (FITC)/propidium iodide (PI) apoptosis detection kit was obtained from MultiSciences (Lianke) Biotech Co., Ltd (Hangzhou, Zhejiang, China). A SYBR[®] Green polymerase chain reaction (PCR) Master Mix was purchased from Applied Biosystems; Thermo Fisher Scientific, Inc. The phosphorylated (p)-p38 and p-c-Jun inhibitors, SB203580 and SP600125, were supplied by Beyotime Institute of Biotechnology (Haimen, China). The PrimeScript Real Time Reagent kit was obtained from Takara Biotechnology Co., Ltd. (Dalian, China).

Antibodies. Primary antibodies against caspase-3 (cat. no. sc-56053), caspase-9 (cat. no. sc-81589), caspase-8 (cat. no. sc-81661), caspase-10 (cat. no. sc-6186), CD95 (cat. no. sc-4276), p53 (cat. no. sc-126), p53-Ser15 (cat. no. sc-101762), p53-Thr18 (cat. no. sc-135631), p53-Ser20 (cat. no. sc-18,079-R), p53-Ser46 (cat. no. sc-101764), p53-Ser392 (cat. no. sc-7997), p-DNA-PK (cat. no. sc-101664), p-ATM (cat. no. sc-47739), p-ATR (cat. no. sc-109912), p-p38 (cat. no. sc-7973), p-c-Jun (cat. no. sc-822) and p-ERK (cat. no. sc-7976) were all purchased from Santa Cruz Biotechnology, Inc. (Dallas, TX, USA). The primary antibody against β -actin, and the IRDye-conjugated anti-rabbit (cat. no. 926-32211), anti-goat (cat. no. 926-32214) and anti-mouse (cat. no. 926-32280) secondary antibodies were purchased from LI-COR Biosciences (Lincoln, NE, USA).

Cell culture. A549 lung cancer cells were supplied by the Cell Bank of Type Culture Collection of the Chinese Academy of Science (Shanghai, China). The A549 cells were grown in DMEM medium supplemented with 10% (v/v) FBS and incubated at 37°C in a humidified (5% CO₂) incubator.

Inhibitor pretreatments. For experiments that included pretreatment with inhibitors of p-p38, p-c-Jun and ROS, A549 cells were pretreated with SB203580 (30 μ M), SP600125 (10 μ M) or APDC (25 μ M) for 30 min at 37°C prior to Aloin (400 μ M) treatment for 48 h at 37°C. Inhibitors were diluted in PBS and added to the cell culture supernatant. After 48 h Aloin treatment, the supernatant was immediately removed and experiments were performed.

Cell proliferation assay. A549 cells were plated into 96-well plates at 5x10³ cells per well. Following incubation for 24 h, the cells were exposed to 0 to 400 μ M concentrations of Aloin. At 24, 48 and 72 h following exposure, the supernatant was removed and 100 μ l (500 μ g/ml) MTT solution was added to each well. Following 4 h of incubation at 37°C, the MTT solution from each well was replaced with 150 μ l dimethyl sulfoxide, which was pipetted up and down several times to dissolve formazan crystals. The optical density was measured at a wavelength of 570 nm for each well using a microtiter

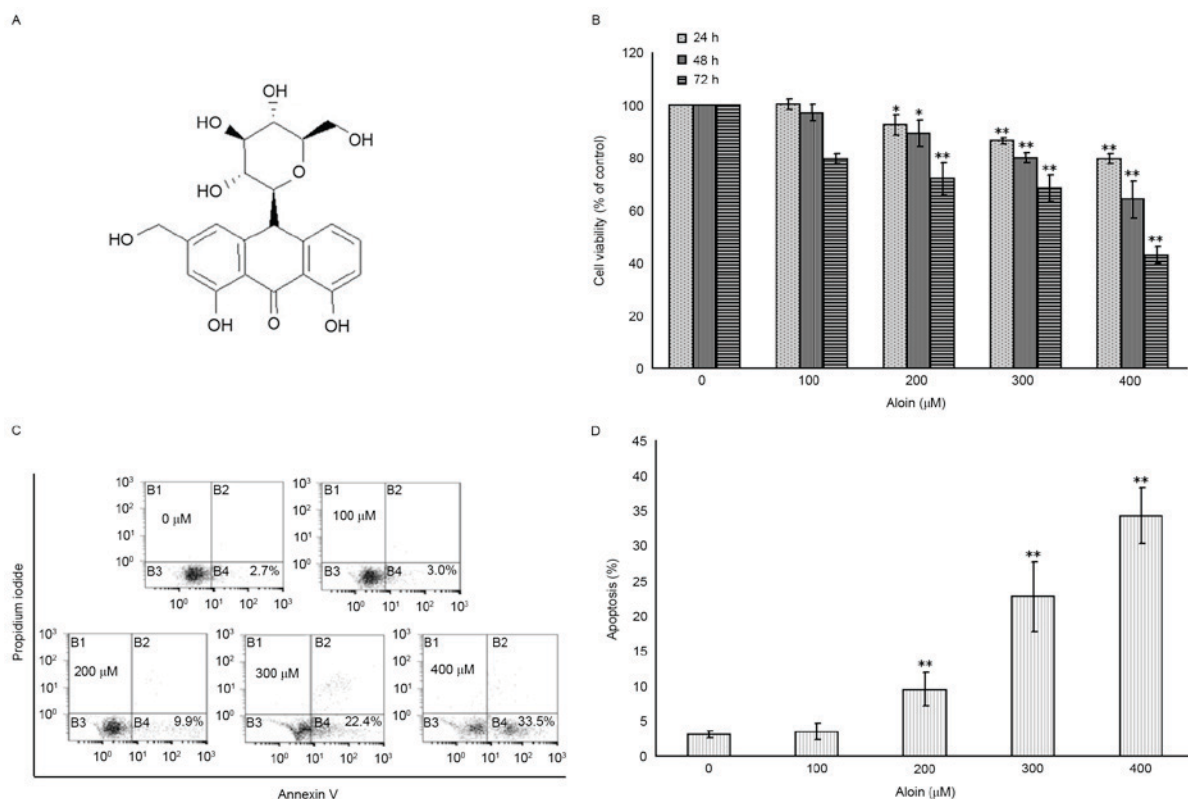


Figure 1. Effects of Aloin on A549 cell proliferation and apoptosis. (A) Chemical structure of Aloin. (B) A549 cells were treated with or without Aloin (0, 100, 200, 300 or 400 μM) for 24, 48 and 72 h, and cell viabilities were then determined by an MTT assay; cell viabilities without Aloin treatment were considered as 100%. (C) A549 cells were treated with or without Aloin (0, 100, 200, 300 and 400 μM) for 48 h, then the percentage of apoptotic cells was analyzed by flow cytometry. (D) Quantification of apoptosis analysis. Data are presented as the mean \pm standard deviation of three independent experiments. * $P < 0.05$ and ** $P < 0.01$ vs. untreated (0 μM) control cells.

plate reader (BioTek Instruments, Inc., Winooski, VT, USA). The results were expressed as the percentage of the control (0 μM Aloin).

Measurement of cell apoptosis. The Annexin V-FITC and PI double staining method was used to analyze the percentage of cells undergoing apoptosis, according to the manufacturer's protocol. Briefly, A549 cells were seeded into 6-well plates at 2×10^5 cells per well. Following incubation with or without the indicated concentrations of Aloin (0 to 400 μM) for 48 h, the cells were trypsinized, washed by PBS, extracted by centrifugation (1,500 \times g for 10 min at 4°C), resuspended in binding buffer containing 1% (v:v) Annexin V-FITC and 2% (v:v) PI and incubated in the dark at room temperature for 20 min. Analysis was performed using a flow cytometer (BD Biosciences, Franklin Lakes, NJ, USA). At least 1×10^5 cells were collected, recorded on a dot plot and analyzed by ModFit v2.0.0 software (Verity Software House, Inc., Topsham, ME, USA).

Western blotting analysis. Expression levels of the target proteins were analyzed by western blotting. Following incubation for 48 h, 1×10^7 A549 cells treated in the presence or absence of Aloin (0 to 400 μM) were harvested and lysed with a radioimmunoprecipitation assay lysis buffer supplied by Beyotime Institute of Biotechnology (20 mM Tris-HCl buffer, pH 7.5, containing 1 mM protease inhibitor mix) for 30 min on ice. Following this, the lysates were centrifuged at 1,500 \times g

for 10 min at 4°C and the supernatant was collected as a whole cell lysate for western blotting analysis. The whole cell lysate (~8 μg) was mixed with a loading buffer [125 mM Tris-HCl, 4% sodium dodecyl sulfate (SDS), 10% sucrose, 0.004% bromophenol blue (BPB) and 10% mercaptoethanol], boiled at 95°C for 5 min and then gel electrophoresis was performed with 8 to 12% SDS-PAGE gels. The protein bands were transferred to polyvinylidene fluoride (PVDF) membranes following manufacturer's protocol (EMD Millipore, Billerica, MA, USA). The PVDF membranes were then blocked with TBS containing 5% non-fat milk at 4°C for 1 h, rinsed with TBS with Tween 20 and incubated with specific primary antibodies, which were diluted in PBS (1:400), at 4°C overnight, followed by the corresponding IRDye-conjugated secondary antibody, which were diluted 1:2,000 in PBS, at room temperature for 1 h. Membranes were detected using an Odyssey Infrared Imaging System and Odyssey v1.3 software (LI-COR Biosciences). The relative optical densities of the target proteins were analyzed using Quantity One software v3.0 (Bio-Rad Laboratories, Inc.). Relative levels of the proteins were normalized to the control b-actin bands in each series and for protein loading. Each test was performed in at least triplicate.

Reverse transcription-quantitative PCR (RT-qPCR). The mRNA expression level of p53 was analyzed by RT-qPCR following incubation of the A549 cells with or without the indicated concentrations of Aloin (0 to 400 μM) for 48 h. Total RNA from $\sim 5 \times 10^6$ cells was isolated using a TRIzol reagent,

and cDNA was synthesized using the PrimeScript Real Time Reagent kit according to the manufacturer's protocol. cDNA amplification was performed at 95°C for 10 sec and 56°C for 30 sec (45 cycles) on a 7500 Real-Time PCR system (Applied Biosystems; Thermo Fisher Scientific, Inc.), using the QuantiTect SYBR® Green PCR kit (Qiagen GmbH, Hilden, Germany) and 2 μ l cDNA, according to the manufacturer's protocol. Specific primers for p53 and β -actin were custom-designed and synthesized by Takara Biotechnology Co., Ltd. The results from three independent experiments are expressed as the n-fold change of untreated (0 μ M) cells and the relative mRNA level of each sample was normalized to β -actin using the $2^{-\Delta\Delta Cq}$ method (29).

Measurement of mitochondrial membrane potential (MMP). MMP was examined by staining A549 cells with rhodamine 123. In healthy cells, rhodamine 123 accumulates and aggregates in the mitochondria; the loss of MMP leads to the release of rhodamine 123 from the mitochondria into the cytosol, increasing intracellular fluorescence (30). Following incubation for 48 h, 5×10^5 cells A549 cells treated with or without the indicated concentrations of Aioin (0 to 400 μ M) were harvested and resuspended in 200 μ l PBS containing 10 μ g/ μ l rhodamine 123 at 37°C for 30 min in the dark. Following staining, the A549 cells were rinsed three times with PBS and analyzed directly by flow cytometry using ModFit software v2.0.0 (Verity Software House, Inc.). The percentage of rhodamine 123 fluorescence positive cells was used to evaluate the extent of mitochondrial depolarization.

Measurement of cytosolic Ca^{2+} level. The level of Ca^{2+} released was measured by staining A549 cells with Fluo-4, which is a fluorescent dye for quantifying the levels of released mitochondrial Ca^{2+} (31). The A549 cells were incubated with or without the indicated concentrations of Aioin (0 to 400 μ M) for 48 h. A total of 1×10^6 cells were harvested and resuspended in 200 μ l PBS containing 2.5 μ M Fluo-4, prior to incubation at 37°C for 30 min in the dark. Following staining, the A549 cells were rinsed three times with PBS and analyzed directly by flow cytometry. The percentage of Fluo-4 fluorescence positive cells was used to evaluate the extent of mitochondrial depolarization.

Measurement of intracellular ROS generation. The generation of ROS was measured by staining A549 cells with a H_2DCF -DA probe, which commonly reacts with a number of ROS molecules including hydrogen peroxide, hydroxyl radicals and peroxynitrite (32). Following incubation for 48 h, 1×10^6 cells A549 cells treated with or without the indicated concentrations of Aioin (0 to 400 μ M) were harvested, resuspended in 200 μ l PBS containing 10 μ M H_2DCF -DA, and incubated at 37°C for 30 min in the dark. Following staining, the A549 cells were rinsed three times with PBS and analyzed directly by flow cytometry using ModFit software v2.0.0 (Verity Software House, Inc.). The percentage of DCFH fluorescence positive cells were used to evaluate the production of ROS.

Statistical analysis. Data are presented as the mean \pm standard deviation. Comparisons among groups were performed using

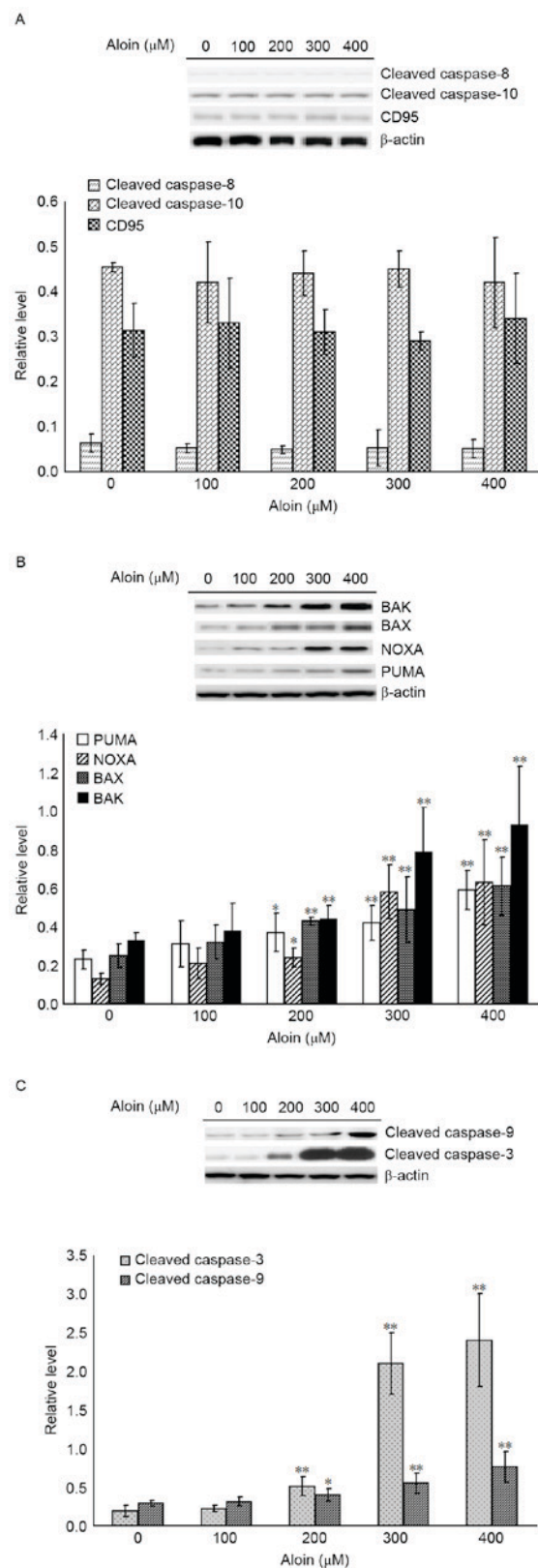


Figure 2. Effects of Aioin on the extrinsic and intrinsic apoptosis pathways. A549 cells were treated with or without Aioin (0, 100, 200, 300 and 400 μ M) for 48 h. Representative western blot images and quantification of protein expression levels of (A) cleaved caspase-8 and -10, and CD95, (B) BAK, BAX, NOXA and PUMA, and (C) cleaved caspase-3 and -9. β -actin served as an internal control. Data are presented as the mean \pm standard deviation. * P <0.05 and ** P <0.01 vs. untreated (0 μ M) control cells. BAK, B-cell lymphoma 2 homologous antagonist killer; BAX, B-cell lymphoma-2 X associated protein; NOXA, phorbol-12-myristate-13-acetate-induced protein 1; PUMA, p53 upregulated modulator of apoptosis; CD95, cluster of differentiation 95.

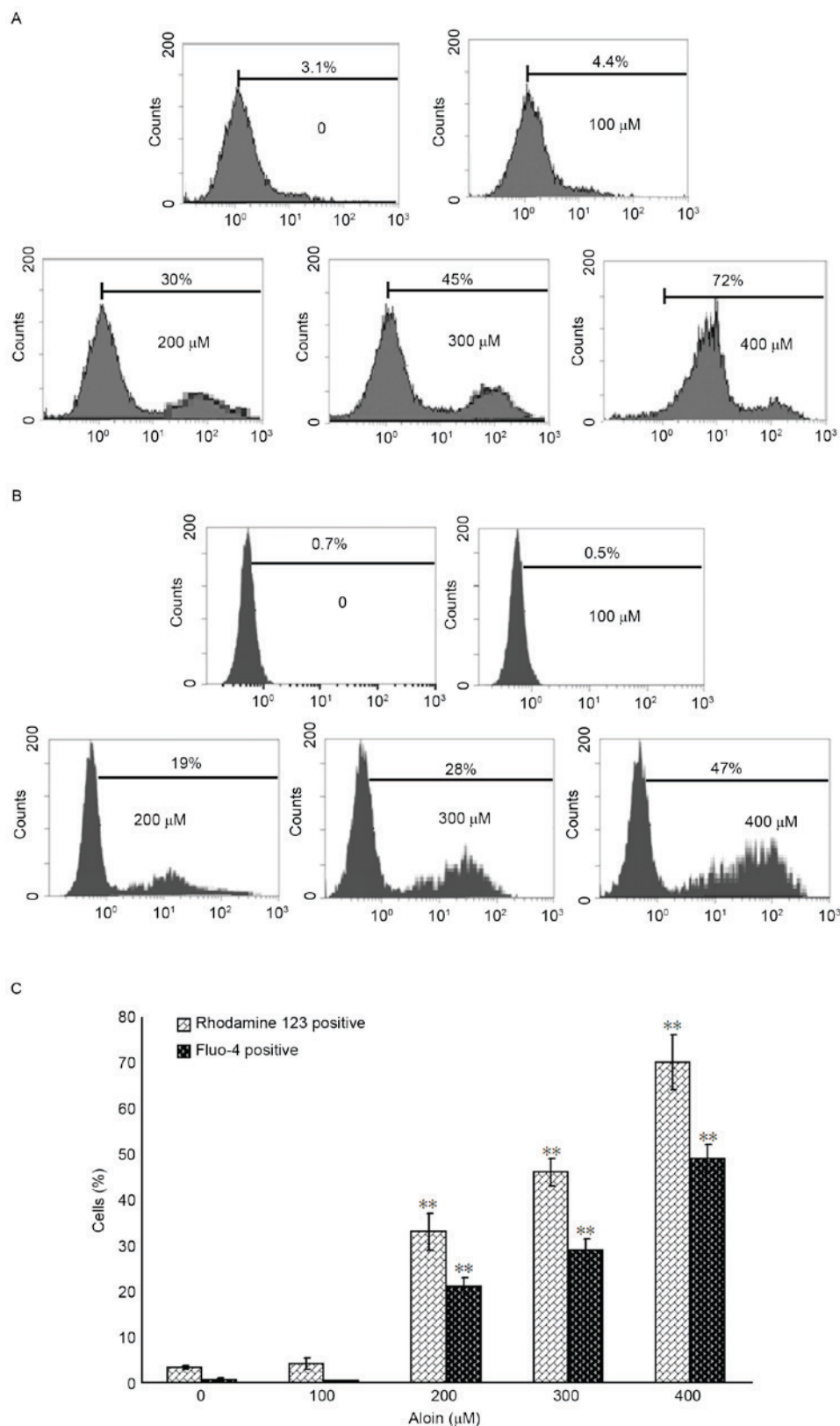


Figure 3. Effects of Aloin on mitochondrial membrane potential and Ca²⁺ levels. A549 cells were treated with or without Aloin (0, 100, 200, 300 or 400 μM) for 48 h. (A) The mitochondrial membrane potential was evaluated using rhodamine 123 staining and flow cytometry. (B) Ca²⁺ levels were monitored using the Fluo-4 fluorescent dye and flow cytometry. (C) Quantification of the three independent experiments performed for (A and B). Data are presented as the mean ± standard deviation of three experiments. *P<0.05 and **P<0.01 vs. untreated (0 μM) control cells.

one-way analysis of variance. If the variation was significant, significant differences between the means of control and of individual Aloin-treated cell groups were analyzed by Fisher's

least significant difference test. P<0.05 was considered to indicate a statistically significant difference. Statistical analysis was performed using SPSS 19.0 (IBM Corp., Armonk, NY, USA).

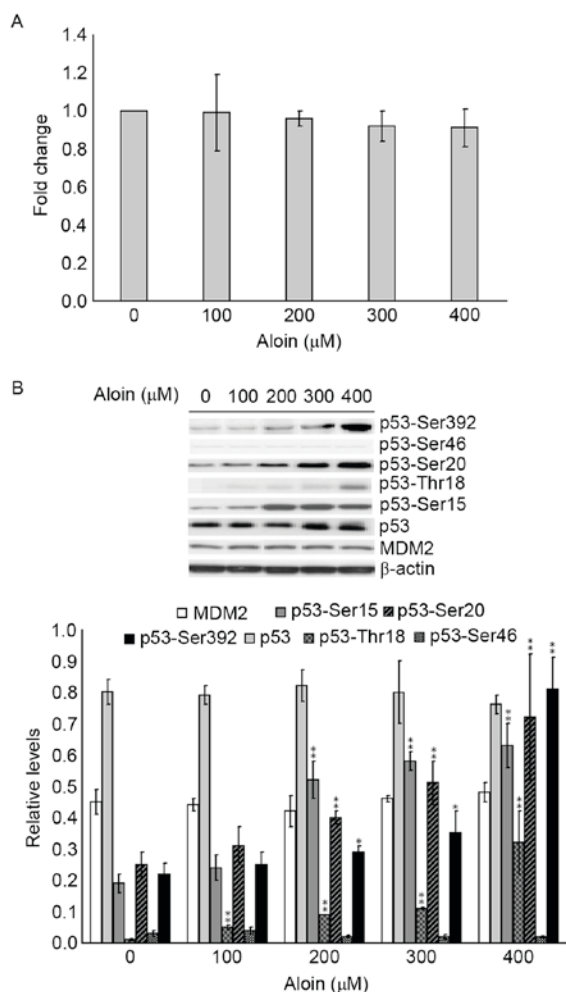


Figure 4. Effects of Aloidin on p53 mRNA and protein expression levels, and p53 phosphorylation. A549 cells were treated with or without Aloidin (0, 100, 200, 300 or 400 μ M) for 48 h. (A) p53 mRNA levels were determined by reverse transcription-quantitative polymerase chain reaction. (B) Representative western blot images and quantification of protein expression levels of MDM2, p53-Ser15, p53-Ser20, p53-Ser392, p53, p53-Thr18 and p53-Ser46 in A549 cells. β -actin served as an internal control. Data are presented as the mean \pm standard deviation. * $P < 0.05$ and ** $P < 0.01$ vs. untreated (0 μ M) control cells. MDM2, mouse double minute 2, Ser, serine; Thr, threonine.

Results

Aloidin induces A549 cell viability inhibition and apoptosis. To evaluate the inhibitory effects of Aloidin on the rate of A549 cell proliferation, cells were exposed to various concentrations (0, 100, 200, 300 and 400 μ M) of Aloidin for 24, 48 and 72 h. As presented in Fig. 1B, Aloidin reduced A549 cell viability in a dose- and time-dependent manner. When compared with the untreated (0 μ M) group, the viabilities of the 200, 300 and 400 μ M Aloidin treated groups were all significantly reduced at the 24, 48 and 72 h time points; however, no significant difference was observed in the cell viabilities at 24, 48 and 72 h for the 100 μ M Aloidin-treated group.

To determine whether the Aloidin-induced inhibition of A549 cell proliferation was the result of apoptosis induction, cell apoptosis was assessed using flow cytometry. As presented in Fig. 1C and D, compared with the untreated group (0 μ M), there was a significant increase in the number of apoptotic

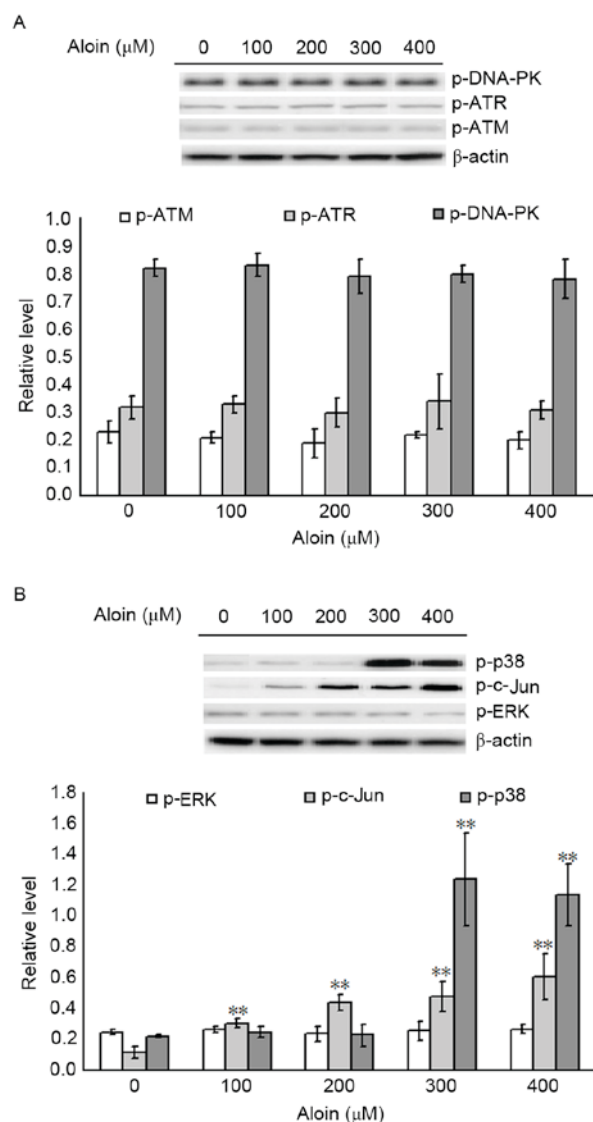


Figure 5. Effects of Aloidin on p53 upstream effectors. A549 cells were treated with or without Aloidin (0, 100, 200, 300 or 400 μ M) for 48 h. Representative western blot images and quantification of (A) p-DNA-PK, p-ATR and p-ATM and (B) p-p38, p-c-Jun and p-ERK protein expression levels in A549 cells. β -actin served as an internal control. Data are presented as the mean \pm standard deviation. ** $P < 0.01$ vs. untreated (0 μ M) control cells. p-, phosphorylated; DNA-PK, DNA-dependent protein kinase; ATR, ataxia-telangiectasia and Rad3 related; ATM, ataxia telangiectasia mutated gene; ERK, extracellular signal-regulated kinase.

A549 cells in the 200, 300 and 400 μ M Aloidin-treated groups at 48 h. However, no significant difference was detected in the level of cell apoptosis in the 100 μ M Aloidin-treated group. Based on these findings, the 48-h time point was selected for further analyses.

Aloidin-induced apoptosis is associated with the intrinsic pathway. To further elucidate the involvement of the apoptosis pathway initiated by Aloidin in A549 cells, the protein expression levels of apoptosis-associated effectors including cleaved caspase-8 and -10, CD95, BAK, BAX, PUMA and NOXA were measured by western blotting. As presented in Fig. 2A, Aloidin treatment failed to induce activation of the extrinsic apoptosis pathway effectors, cleaved-caspase-8 and -10, and CD95.

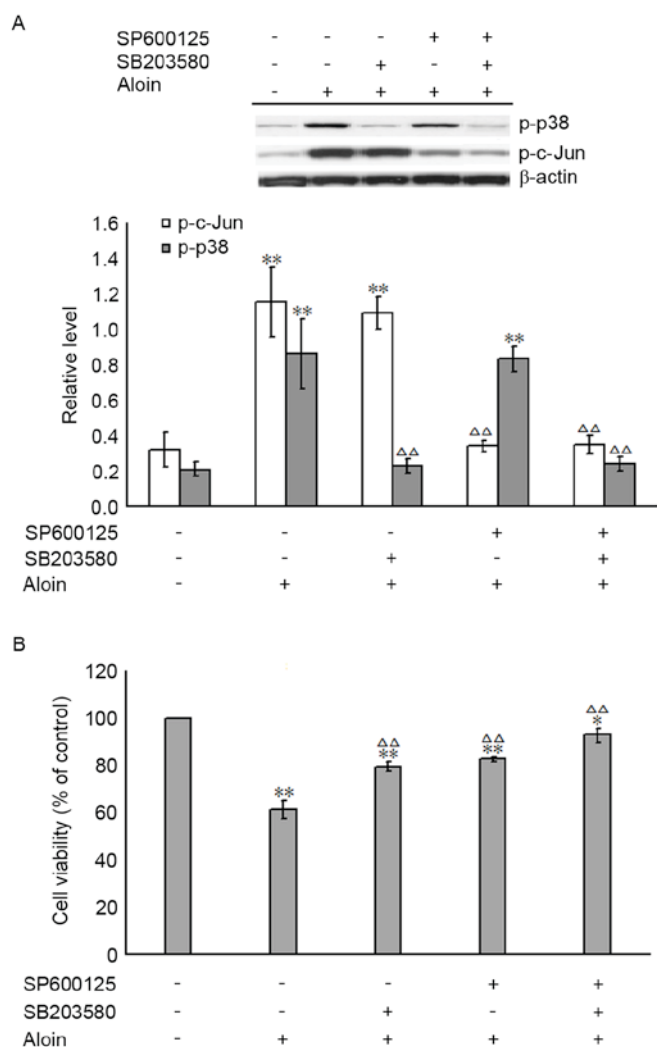


Figure 6. p38 and c-Jun activities in Alain-induced A549 cell viability. A549 cells were pretreated with or without 30 μ M SB203580 and 10 μ M SP600125, alone or in combination, for 30 min, then incubated with or without 400 μ M Alain for 48 h. (A) Representative western blot images and quantification of protein expression levels of p-p38 and p-c-Jun. β -actin served as an internal control. (B) A549 cell viabilities were determined by an MTT assay; the cell viabilities without SB203580, SP600125 and Alain treatment were considered as 100%. Data are presented as the mean \pm standard deviation. * P <0.05 and ** P <0.01 vs. untreated (0 μ M) control cells; $\Delta\Delta P$ <0.01 vs. Alain only treatment.

However, compared with the untreated (0 μ M) group, treatment with 200, 300 and 400 μ M Alain significantly increased the protein expression levels of the intrinsic apoptosis pathway effectors, BAK, BAX, PUMA and NOXA (Fig. 2B). In addition, as presented in Fig. 2C, treatment with 200, 300 and 400 μ M Alain also significantly increased the protein expression levels of cleaved caspase-3 and -9, which are downstream effectors of the intrinsic and extrinsic apoptosis pathways.

Alain induces the loss of MMP and release of mitochondrial Ca^{2+} . To further define the role of the mitochondria in Alain-induced A549 cell apoptosis, the MMP and levels of released mitochondrial Ca^{2+} were determined using flow cytometry. When compared with the untreated (0 μ M) group, treatment with 200, 300 and 400 μ M Alain induced a significant disruption in the MMP and release of mitochondrial

Ca^{2+} , as indicated by the observed increase in the percentage of rhodamine 123 or Fluo-4 positive A549 cells, respectively (Fig. 3).

Alain induces activation of p53 phosphorylation. It was hypothesized that Alain-induced A549 cell apoptosis may be p53-dependent. To investigate this, the levels of p53 mRNA were measured using RT-qPCR. As presented in Fig. 4A, 100 to 400 μ M Alain did not exert any directly inductive or inhibitory effects on p53 mRNA expression following treatment for 48 h. Following this, the roles of Alain in the protein expression of p53 and its antagonist MDM2, and p53 protein phosphorylation status, were investigated. As presented in Fig. 4B, compared with the untreated (0 μ M) group, there were no detectable differences in the protein expression levels of p53, MDM2 or p53-Ser46. In contrast, treatment with 200, 300 and 400 μ M Alain resulted in strong activation of p53-Ser15, p53-Thr18, p53-Ser20 and p53-Ser392. These observations indicated that the signaling system responsible for p53 phosphorylation of Ser15, Thr18, Ser-20 and Ser-392 was involved in Alain-induced apoptosis in A549 cells.

p38 and c-Jun are responsible for Alain-induced p53 phosphorylation. As DNA-PK and MAPKs are traditionally phosphokinases responsible for p53 phosphorylation, the extent of DNA-PK (p-ATM, p-ATR and p-DNA-PK) and MAPK (p-p38, p-c-Jun and p-ERK) activation in A549 cells following Alain exposure were examined. As presented in Fig. 5A, when compared with the untreated (0 μ M) group, treatment with 100 to 400 μ M Alain did not alter the levels of p-ATM, p-ATR and p-DNA-PK. However, when compared with untreated (0 μ M) groups, treatment with 100 to 400 μ M and 300 to 400 μ M Alain for 48 h significantly increased p-c-Jun and p-p38 levels, respectively. In addition, Alain treatment did not alter the protein expression levels of p-ERK. These results suggest that c-Jun and/or p38-mediated cell signaling pathways may contribute to Alain activities in p53 phosphorylation.

Inhibition of p-p38 and/or p-c-Jun attenuates the effect of Alain on A549 cell viability. To determine whether Alain-induced A549 cell death is attributable to the activation of p-p38 and/or p-c-Jun MAPKs, the specific inhibitors of p-p38 and p-c-Jun, SB203580 (30 μ M) and SP600125 (10 μ M), were used to pre-treat A549 cells for 30 min. The inhibiting efficiencies of SB203580 and SP600125 are shown in Fig. 6A. The levels of p-p38 and p-c-Jun in the SB203580 and SP600125 pretreated groups were significantly reduced when compared with the group treated with 400 μ M Alain only; the levels observed were nearly equal to those of the untreated group (0 μ M Alain). The impact of SB203580 and SP600125 on Alain-induced A549 cell death was evaluated by MTT assay. As presented in Fig. 6B, SB203580 and SP600125 pretreatment, alone or in combination, significantly attenuated the Alain-induced decrease in A549 cell viabilities. These results further support the hypothesis that Alain-induced A549 cell apoptosis is associated with the c-Jun- and p38-mediated cell signaling pathways.

Alain induces ROS production in A549 cells. It has been widely reported that the generation of ROS induces the activation of MAPKs and subsequently, apoptosis (33,34). To investigate

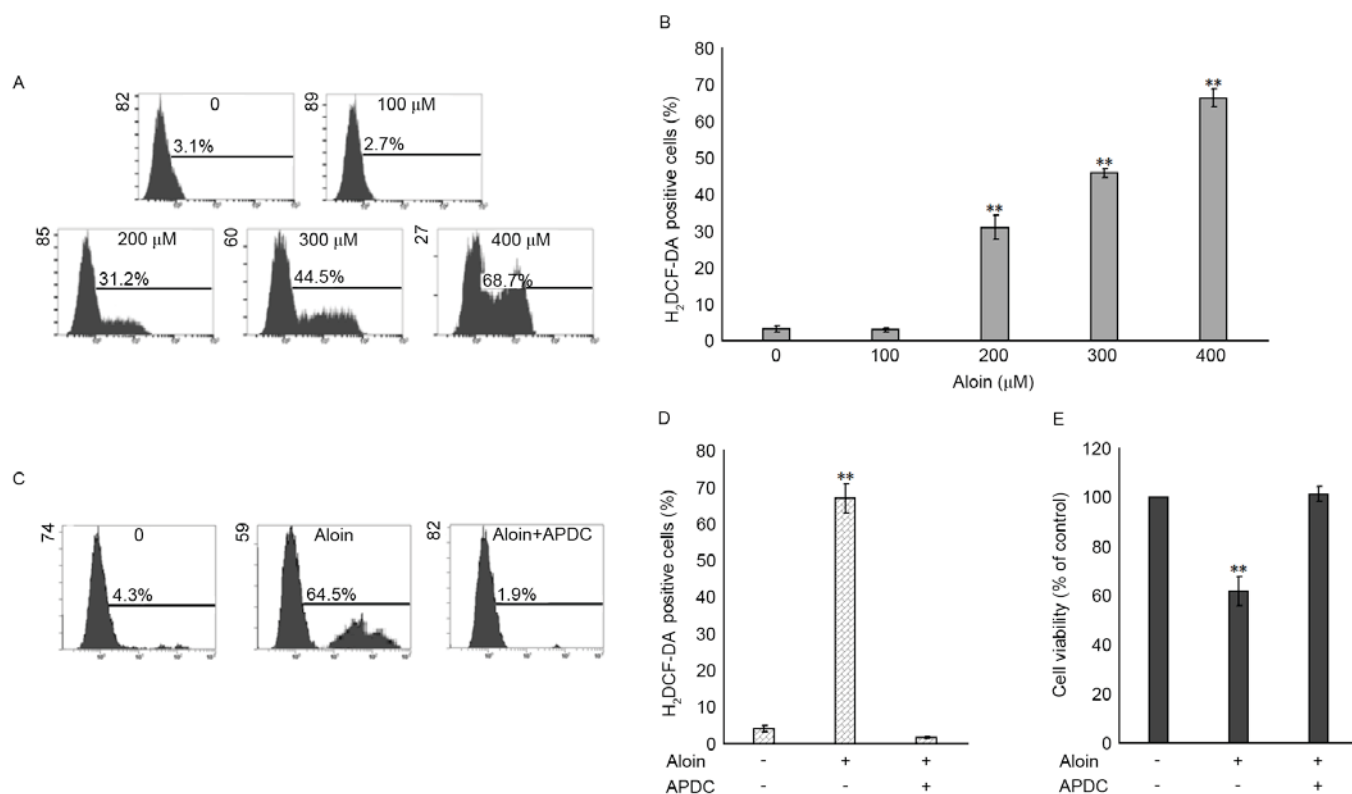


Figure 7. Effects of Aloin on ROS production. (A) A549 cells were treated with or without Aloin (0, 100, 200, 300 and 400 μ M) for 48 h. Flow cytometric analysis and (B) quantification of ROS production. (C) A549 cells were pre-treated with or without 25 μ M antioxidant APDC for 30 min and the cells were then treated with or without 400 μ M Aloin for 48 h. (D) Flow cytometric analysis and (E) quantification of ROS production. (E) A549 cells were pre-treated with or without 25 μ M APDC for 30 min, followed by and treatment with or without 400 μ M Aloin for 48 h. Cell viability was determined by an MTT assay; cell viabilities without Aloin treatment were considered as 100%. Data are presented as the mean \pm standard deviation of three independent experiments. ** $P < 0.01$ vs. untreated (0 μ M) control cells. ROS, reactive oxygen species; H₂DCF-DA, dichlorodihydrofluorescein diacetate; APDC, 4-aminopyrrolidine-2,4-dicarboxylic acid.

whether ROS generation is associated with Aloin-induced activation of c-Jun and p38, and apoptosis, the levels of ROS in Aloin-treated A549 cells were evaluated by flow cytometry following 48 h incubation and H₂DCF-DA probe labeling. As presented in Fig. 7A and B, when compared with the untreated (0 μ M) group, treatment with 200, 300 and 400 μ M Aloin induced a significant accumulation of ROS. To further define the role of ROS in the Aloin-induced decrease in cell viability, the ROS inhibitor, APDC (25 μ M), was used for A549 cell pretreatment for 30 min. As presented in Fig. 7C and D, APDC pretreatment inhibited the 400 μ M Aloin-induced generation of ROS in A549 cells. When compared with the untreated group, APDC pretreatment attenuated the 400 μ M Aloin-induced inhibition of A549 cell viability (Fig. 7E). These results indicated that ROS generation may serve a crucial role in Aloin-induced apoptosis.

Discussion

Aloin, the main active component of aloe, has long been used in traditional Chinese medicine. However, it has been reported to induce apoptosis in a number of different cancer cell types (2,3). In agreement with these previous studies, the present study demonstrated that Aloin at concentrations of 200 to 400 μ M significantly inhibited the proliferation rates of A549 cells 48 h post-treatment. These results were further confirmed by flow cytometric analysis, which demonstrated

that 200 to 400 μ M Aloin increased apoptosis in A549 cells following treatment for 48 h.

ROS have the ability to interact with cellular proteins, lipids and DNA, resulting in oxidative stress, which in turn stimulates extrinsic and/or intrinsic apoptosis (35,36). ROS may also serve as cell signaling molecules and cause damage to foreign bodies (37). Overproduction of ROS may be induced by a number of intra- and extracellular stressors (38-40). In the present study, the production of ROS in Aloin-treated A549 cells was evaluated. Elevated ROS levels were concurrent with the increased level of apoptosis. The results indicated that the elevation in ROS may be an important initial cellular event that occurs during Aloin-induced apoptosis. This was further confirmed by experiments using the specific ROS inhibitor, APDC, which attenuated the Aloin-induced inhibition of cell proliferation. These results, coupled with the disruption of the MMP, increased levels of cytosolic Ca²⁺ and activation of BAK, BAX, PUMA and NOXA, suggested that the accumulation of ROS contributes to the induction of mitochondria-dependent cell apoptosis under these experimental conditions. These observations further confirmed the hypothesis that chemotherapeutic agents may be selectively toxic to tumor cells as they increase oxidative stress to cells and induce apoptosis.

p53 may be activated by oncogene expression, DNA damage and oxidative stress (41,42). Under these conditions, phosphorylation of its N-terminus residues may stabilize p53

and activate its anticancer activity via the intrinsic and/or extrinsic apoptosis pathways (43,44). In the present study, key observations were made concerning the phosphorylation of p53 on the Ser15, Thr18, Ser20, Ser46 and Ser392 residues. With the concentrations that induced apoptosis, Aloin exposure increased p53-Ser15, p53-Thr18, p53-Ser20 and p53-Ser392 protein expression levels, whereas phosphorylation of Ser46 was not induced. In contrast, in Aloin-treated A549 cells, the mRNA and protein expression levels of p53 were not increased. Phosphorylation of Ser-15, -20 and -392, and Thr18, alone or in combination, may be induced in response to a number of chemotherapeutic agents, including camptothecin, cisplatin and ionizing radiation (45-49). Therefore, the present study demonstrated that Aloin also induces the phosphorylation of the p53 protein on Ser-15, -20 and -392, and Thr18. The specific roles of each phosphorylated residue requires further determination.

MDM2, as a target gene of p53, inhibits p53-induced transactivation by inducing ubiquitination of the p53 N-terminus and serving as a E3 ubiquitin ligase to mark p53 for rapid degradation (5,50). In addition, MDM2 has p53-independent anti-apoptotic functions (50,51), and amplification of MDM2 genes or overexpression of the MDM2 protein are features of a number of tumor types (41). Thus, developing treatments to reduce the levels of MDM2 may be viable strategies for cancer therapy. Specific alkylating agents used in cancer chemotherapy treatments have been reported to downregulate the expression of MDM2 (52-54). For example, the DNA alkylating agents mitomycin C and methylmethane sulfonate, induced a reduction in MDM2 protein expression in RKO cells. These decreased levels of MDM2 coincided with the downregulation of ubiquitinated p53 and p53/MDM2 binding complexes (54). In another study, triptolide, a natural product with anticancer properties, induced apoptosis in lymphoblastic leukemia cells by inhibiting the MDM2-XIAP cell signaling pathway (55). However, in the present study, the expression of MDM2 in Aloin-treated A549 cells was not altered. Together with the findings of previous studies, these results indicated that inhibition of MDM2 may be cell-type-specific and/or stress-type-dependent events.

The MAPK family includes c-Jun, p38 and ERKs (56). Among the MAPK family, activation of ERKs is usually involved in cell survival or differentiation, whereas activation of c-Jun and p38 are commonly associated with promoting cell apoptosis and death, particularly under oxidative-stress conditions (57). In addition, phosphorylation of p53 may be mediated by c-Jun and p38 (17,58). Consistent with previous studies, the present study demonstrated that c-Jun and p38 were essential for the Aloin-induced inhibition of cell proliferation. This was further confirmed by pretreatment with c-Jun and the p38 MAPK specific inhibitors, SP600125 and SB203580, alone or in combination, which significantly attenuated the Aloin-induced inhibition of cell proliferation. However, the interactions between c-Jun and p38, and p53 phosphorylation, require further investigation in future studies.

In conclusion, the present study demonstrated that Aloin treatment induces ROS accumulation in A549 cells, which in turn triggers apoptosis via the intrinsic pathway. Aloin-induced apoptosis was associated with p53 phosphorylation and was dependent on c-Jun and p38 activation. These results provided

mechanistic insight into the therapeutic potential of Aloin in clinical treatments for lung cancer; however, further study is required to confirm these mechanisms *in vivo*.

Acknowledgements

This study was supported by a grant from the National Natural Science Foundation (grant no. 81000032).

References

- Gutterman Y and Chausser-Volfson E: The content of secondary phenol metabolites in pruned leaves of *Aloe arborescens*, a comparison between two methods: Leaf exudates and leaf water extract. *J Nat Med* 62: 430-435, 2008.
- Tabolacci C, Rossi S, Lentini A, Provenzano B, Turcano L, Facchiano F and Beninati S: Aloin enhances cisplatin antineoplastic activity in B16-F10 melanoma cells by transglutaminase-induced differentiation. *Amino Acids* 44: 293-300, 2013.
- Buenz EJ: Aloin induces apoptosis in Jurkat cells. *Toxicol In Vitro* 22: 422-429, 2008.
- Pronin AN, Xu H, Tang H, Zhang L, Li Q and Li X: Specific alleles of bitter receptor genes influence human sensitivity to the bitterness of aloin and saccharin. *Curr Biol* 16: 1403-1408, 2007.
- Michael D and Oren M: The p53 and Mdm2 families in cancer. *Curr Opin Genet Dev* 12: 53-59, 2002.
- Jiang Y, Rao K, Yang G, Chen X, Wang Q, Liu A, Zheng H and Yuan J: Benzo(a)pyrene induces p73 mRNA expression and necrosis in human lung adenocarcinoma H1299 cells. *Environ Toxicol* 27: 202-210, 2012.
- Callén E, Jankovic M, Wong N, Zha S, Chen HT, Difilippantonio S, Di Virgilio M, Heidkamp G, Alt FW, Nussenzweig A and Nussenzweig M: Essential role for DNA-PKcs in DNA double-strand break repair and apoptosis in ATM-deficient lymphocytes. *Mol Cell* 34: 285-297, 2009.
- Saxena N, Ansari KM, Kumar R, Dhawan A, Dwivedi PD and Das M: Patulin causes DNA damage leading to cell cycle arrest and apoptosis through modulation of Bax, p(53) and p(21/WAF1) proteins in skin of mice. *Toxicol Appl Pharmacol* 234: 192-201, 2009.
- Sheikh MS and Fornace AJ Jr: Role of p53 family members in apoptosis. *J Cell Physiol* 182: 171-181, 2000.
- Wang C, Gao C, Chen Y, Yin J, Wang P and Lv X: Expression pattern of the apoptosis-stimulating protein of p53 family in p53+ human breast cancer cell lines. *Cancer Cell International* 13: 116, 2013.
- Deb SP, Singh S and Deb S: MDM2 overexpression, activation of signaling networks and cell proliferation. *Subcell Biochem* 85: 215-234, 2014.
- Krzyszniak M, Zajkowicz A, Matuszczyk I and Rusin M: Rapamycin prevents strong phosphorylation of p53 on serine 46 and attenuates activation of the p53 pathway in A549 lung cancer cells exposed to actinomycin D. *Mech Ageing Dev* 139: 11-21, 2014.
- Jabbur JR, Huang P and Zhang W: DNA damage-induced phosphorylation of p53 at serine 20 correlates with p21 and Mdm-2 induction in vivo. *Oncogene* 19: 6203-6208, 2000.
- Tichý A, Zášková D, Zoelzer F, Vávrová J, Sinkorová Z, Pejchal J, Osterreicher J and Rezáčová M: Gamma-radiation-induced phosphorylation of p53 on serine 15 is dose-dependent in MOLT-4 leukaemia cells. *Folia Biol (Praha)* 55: 41-44, 2009.
- Tampio M, Loikkanen J, Myllynen P, Mertanen A and Vahakangas KH: Benzo(a)pyrene increases phosphorylation of p53 at serine 392 in relation to p53 induction and cell death in MCF-7 cells. *Toxicol Lett* 178: 152-159, 2008.
- Sluss HK, Armata H, Gallant J and Jones SN: Phosphorylation of serine 18 regulates distinct p53 functions in mice. *Mol Cell Biol* 24: 976-984, 2004.
- Lee KB, Kim KR, Huh TL and Lee YM: Proton induces apoptosis of hypoxic tumor cells by the p53-dependent and p38/JNK MAPK signaling pathways. *Int J Oncol* 33: 1247-1256, 2008.
- Brown L and Benchimol S: The involvement of MAPK signaling pathways in determining the cellular response to p53 activation: Cell cycle arrest or apoptosis. *J Biol Chem* 281: 3832-3840, 2006.

19. Huang J, Wu L, Tashiro S, Onodera S and Ikejima T: Reactive oxygen species mediate oridonin-induced HepG2 apoptosis through p53, MAPK and mitochondrial signaling pathways. *J Pharmacol Sci* 107: 370-379, 2008.
20. Salles-Passador I, Fotedar A and Fotedar R: Cellular response to DNA damage. Link between p53 and DNA-PK. *C R Acad Sci III* 322: 113-120, 1999.
21. Gatz SA, Keimling M, Baumann C, Dörk T, Debatin KM, Fulda S and Wiesmüller L: Resveratrol modulates DNA double-strand break repair pathways in an ATM/ATR-p53- and -Nbs1-dependent manner. *Carcinogenesis* 29: 519-527, 2008.
22. Chène P: Inhibiting the p53-MDM2 interaction: An important target for cancer therapy. *Nat Rev Cancer* 3: 102-109, 2003.
23. Huang X, Wu Z, Mei Y and Wu M: XIAP inhibits autophagy via XIAP-Mdm2-p53 signalling. *EMBO J* 32: 2204-2216, 2013.
24. Zheng M, Yang J, Xu X, Sebolt JT, Wang S and Sun Y: Efficacy of MDM2 inhibitor MI-219 against lung cancer cells alone or in combination with MDM2 knockdown, a XIAP inhibitor or etoposide. *Anticancer Res* 30: 3321-3331, 2010.
25. Lan YH, Chiang JH, Huang WW, Lu CC, Chung JG, Wu TS, Jhan JH, Lin KL, Pai SJ, Chiu YJ, *et al*: Activations of both extrinsic and intrinsic pathways in HCT 116 human colorectal cancer cells contribute to apoptosis through p53-Mediated ATM/Fas signaling by emilia sonchifolia extract, a folklore medicinal plant. *Evid Based Complement Alternat Med* 2012: 178178, 2012.
26. Seitz SJ, Schleithoff ES, Koch A, Schuster A, Teufel A, Staib F, Stremmel W, Melino G, Krammer PH, Schilling T and Müller M: Chemotherapy-induced apoptosis in hepatocellular carcinoma involves the p53 family and is mediated via the extrinsic and the intrinsic pathway. *Int J Cancer* 126: 2049-2066, 2010.
27. Liu T, Laurell C, Selivanova G, Lundeberg J, Nilsson P and Wiman KG: Hypoxia induces p53-dependent transactivation and Fas/CD95-dependent apoptosis. *Cell Death Differ* 14: 411-421, 2007.
28. Lee MC, Liao JD, Huang WL, Jiang FY, Jheng YZ, Jin YY and Tseng YS: Aloin-induced cell growth arrest, cell apoptosis, and autophagy in human non-small cell lung cancer cells. *Biomarkers and Genomic Medicine* 6: 144-149, 2014.
29. Livak KJ and Schmittgen TD: Analysis of relative gene expression data using real time quantitative PCR and the 2(-Delta Delta C(T)) method. *Methods* 25: 402-408, 2001.
30. Camins A, Sureda FX, Gabriel C, Pallàs M, Escubedo E and Camarasa J: Modulation of neuronal mitochondrial membrane potential by the NMDA receptor: Role of arachidonic acid. *Brain Res* 777: 69-74, 1997.
31. Cao XH, Zhao SS, Liu DY, Wang Z, Niu LL, Hou LH and Wang CL: ROS-Ca(2+) is associated with mitochondria permeability transition pore involved in surfactin-induced MCF-7 cells apoptosis. *Chem Biol Interact* 190: 16-27, 2011.
32. Liu J, Chang F, Li F, Fu H, Wang J, Zhang S, Zhao J and Yin D: Palmitate promotes autophagy and apoptosis through ROS-dependent JNK and p38 MAPK. *Biochem Biophys Res Commun* 463: 262-267, 2015.
33. Sato A, Okada M, Shibuya K, Watanabe E, Seino S, Narita Y, Shibui S, Kayama T and Kitanaka C: Pivotal role for ROS activation of p38 MAPK in the control of differentiation and tumor-initiating capacity of glioma-initiating cells. *Stem Cell Res* 12: 119-131, 2014.
34. Liu WH, Cheng YC and Chang LS: ROS-mediated p38alpha MAPK activation and ERK inactivation responsible for upregulation of Fas and FasL and autocrine Fas-mediated cell death in Taiwan cobra phospholipase A(2)-treated U937 cells. *J Cell Physiol* 219: 642-651, 2009.
35. Colin DJ, Limagne E, Ragot K, Lizard G, Ghiringhelli F, Solary É, Chauffert B, Latruffe N and Delmas D: The role of reactive oxygen species and subsequent DNA-damage response in the emergence of resistance towards resveratrol in colon cancer models. *Cell Death Dis* 5: e1533, 2014.
36. Lapidus RG, Carter-Cooper BA, Sadowska M, Choi EY, Wonodi O, Muvarak N, Natarajan K, Pidugu LS, Jaiswal A, Toth EA, *et al*: Hydroxylated dimeric naphthoquinones increase the generation of reactive oxygen species, induce apoptosis of acute myeloid leukemia cells and are not substrates of the multidrug resistance proteins abcb1 and abcg2. *Pharmaceuticals (Basel)* 9: pii: E4, 2016.
37. Hsieh CJ, Kuo PL, Hsu YC, Huang YF, Tsai EM and Hsu YL: Arctigenin, a dietary phytoestrogen, induces apoptosis of estrogen receptor-negative breast cancer cells through the ROS/p38 MAPK pathway and epigenetic regulation. *Free Radic Biol Med* 67: 159-170, 2014.
38. Sanada M, Kuroda K and Ueda M: ROS production and apoptosis induction by formation of Gts1p-mediated protein aggregates. *Biosci Biotechnol Biochem* 75: 1546-1553, 2011.
39. Derouet-Humbert E, Drăgan CA, Hakki T and Bureik M: ROS production by adrenodoxin does not cause apoptosis in fission yeast. *Apoptosis* 12: 2135-2142, 2007.
40. Jiang H, Hou C, Zhang S, Xie H, Zhou W, Jin Q, Cheng X, Qian R and Zhang X: Matrine upregulates the cell cycle protein E2F-1 and triggers apoptosis via the mitochondrial pathway in K562 cells. *Eur J Pharmacol* 559: 98-108, 2007.
41. Pei D, Zhang Y and Zheng J: Regulation of p53: A collaboration between Mdm2 and Mdmx. *Oncotarget* 3: 228-235, 2012.
42. Walker G and Box N: Ribosomal stress, p53 activation and the tanning response. *Expert Rev Dermatol* 3: 649-656, 2008.
43. Yang J, Ahmed A and Ashcroft M: Activation of a unique p53-dependent DNA damage response. *Cell Cycle* 8: 1630-1632, 2009.
44. Pabla N, Huang S, Mi QS, Daniel R and Dong Z: ATR-Chk2 signaling in p53 activation and DNA damage response during cisplatin-induced apoptosis. *J Biol Chem* 283: 6572-6583, 2008.
45. Cheng F, Liu J, Teh C, Chong SW, Korzh V, Jiang YJ and Deng LW: Camptothecin-induced downregulation of MLL5 contributes to the activation of tumor suppressor p53. *Oncogene* 30: 3599-3611, 2011.
46. Fraser M, Bai T and Tsang BK: Akt promotes cisplatin resistance in human ovarian cancer cells through inhibition of p53 phosphorylation and nuclear function. *Int J Cancer* 122: 534-546, 2008.
47. Katayama A, Ogino T, Bandoh N, Takahara M, Kishibe K, Nonaka S and Harabuchi Y: Overexpression of small ubiquitin-related modifier-1 and sumoylated Mdm2 in oral squamous cell carcinoma: Possible involvement in tumor proliferation and prognosis. *Int J Oncol* 31: 517-524, 2007.
48. Saito S, Goodarzi AA, Higashimoto Y, Noda Y, Lees-Miller SP, Appella E and Anderson CW: ATM mediates phosphorylation at multiple p53 sites, including Ser(46), in response to ionizing radiation. *J Biol Chem* 277: 12491-12494, 2002.
49. Yamauchi M, Suzuki K, Kodama S and Watanabe M: Stabilization of alanine substituted p53 protein at Ser15, Thr18, and Ser20 in response to ionizing radiation. *Biochem Biophys Res Commun* 323: 906-911, 2004.
50. Momand J, Villegas A and Belyi VA: The evolution of MDM2 family genes. *Gene* 486: 23-30, 2011.
51. Ongkeko WM, Wang XQ, Siu WY, Lau AW, Yamashita K, Harris AL, Cox LS and Poon RY: MDM2 and MDMX bind and stabilize the p53-related protein p73. *Curr Biol* 9: 829-832, 1999.
52. Youu MS, Park CL, Kim MH, Kim HM and Jeong HJ: Inhibition of MDM2 expression by rosmarinic acid in TSLP-stimulated mast cell. *Eur J Pharmacol* 771: 191-198, 2016.
53. Kao CL, Hsu HS, Chen HW and Cheng TH: Rapamycin increases the p53/MDM2 protein ratio and p53-dependent apoptosis by translational inhibition of mdm2 in cancer cells. *Cancer Lett* 286: 250-259, 2009.
54. Inoue T, Geyer RK, Yu ZK and Maki CG: Downregulation of MDM2 stabilizes p53 by inhibiting p53 ubiquitination in response to specific alkylating agents. *FEBS Lett* 490: 196-201, 2001.
55. Huang M, Zhang H, Liu T, Tian D, Gu L and Zhou M: Triptolide inhibits MDM2 and induces apoptosis in acute lymphoblastic leukemia cells through a p53-independent pathway. *Mol Cancer Ther* 12: 184-194, 2013.
56. Vitale I, Senovilla L, Galluzzi L, Criollo A, Vivet S, Castedo M and Kroemer G: Chk1 inhibition activates p53 through p38 MAPK in tetraploid cancer cells. *Cell Cycle* 7: 1956-1961, 2008.
57. Zhang JQ, Li YM, Liu T, He WT, Chen YT, Chen XH, Li X, Zhou WC, Yi JF and Ren ZJ: Antitumor effect of matrine in human hepatoma G2 cells by inducing apoptosis and autophagy. *World J Gastroenterol* 16: 4281-4290, 2010.
58. Taylor CA, Zheng Q, Liu Z and Thompson JE: Role of p38 and JNK MAPK signaling pathways and tumor suppressor p53 on induction of apoptosis in response to Ad-eIF5A1 in A549 lung cancer cells. *Mol Cancer* 12: 35, 2013.